

*dr Michał Zawada*

Opracowanie utworu pod tytułem:

***"Diagnostic and imaging of cold atoms" w ramach kursu zaawansowanego, organizowanego dniach 31.08 - 25.09.09 będącego kontynuacją szkoleń z zakresu eksploatacji i zarządzania dużą infrastrukturą badawczą organizowanego przez Narodowe Laboratorium Technologii Kwantowych***



INNOWACYJNA GOSPODARKA  
NARODOWA TECHNOLOGICZNA SYNERGIA

Projekt współfinansowany ze środków Europejskiego Funduszu Rozwoju Regionalnego w ramach Programu Operacyjnego Innowacyjna Gospodarka



UNIA EUROPEJSKA  
ROZWOJ I WYKONANIE  
INICJATYW



Narodowe  
Laboratorium  
Technologii  
Kwantowych

Projekt współfinansowany ze środków Europejskiego Funduszu  
Rozwoju Regionalnego w ramach Programu Operacyjnego  
Innowacyjna Gospodarka



**INNOWACYJNA GOSPODARKA**  
NARODOWA STRATEGIA SPÓJNOŚCI

**UNIA EUROPEJSKA**  
EUROPEJSKI FUNDUSZ  
ROZWOJU REGIONALNEGO



Imaging  
Small beam techniques  
No beam at all  
Back to the BEC



Diagnostic and imaging of cold atoms

**FAMO**  
**MT BEC GROUP**



INNOWACYJNA GOSPODARKA  
NARODOWA STRATEGIA SPÓJNOŚCI

UNIA EUROPEJSKA  
EUROPEJSKI FUNDUSZ  
ROZWOJU REGIONALNEGO



Diagnostic and imaging of cold atoms

# How to probe Bose-Einstein condensate

## Everything

we know about gaseous Bose-Einstein condensate has been obtained by optical diagnostics

Any contact probe would be way too big!



# How to probe Bose-Einstein condensate

## The interaction of atoms with a beam of light:

- spontaneous absorption of photons
- re-emission of photons
- shifting the phase of transmitting light



# How to probe Bose-Einstein condensate

## The interaction of atoms with a beam of light:

- spontaneous absorption of photons - absorptive imaging
- re-emission of photons
- shifting the phase of transmitting light



# How to probe Bose-Einstein condensate

## The interaction of atoms with a beam of light:

- spontaneous absorption of photons - **absorptive imaging**
- re-emission of photons - **fluorescence imaging**
- shifting the phase of transmitting light



# How to probe Bose-Einstein condensate

## The interaction of atoms with a beam of light:

- spontaneous absorption of photons - absorptive imaging
- re-emission of photons - fluorescence imaging
- shifting the phase of transmitting light - dispersive imaging



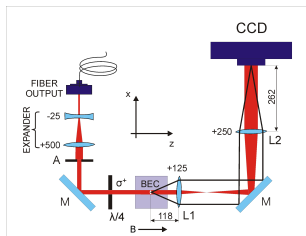


# Outline

- 1 **Imaging**
  - Absorption Imaging
  - Phase-contrast and polarisation-contrast imaging
  - Fluorescence
- 2 **Small beam techniques**
  - Time of flight
  - Pump-probe spectroscopy in an operating trap
  - FWM
- 3 **No beam at all**
  - Release and recapture
  - Parametric resonance
  - Studies of the cold atoms collisions
- 4 **Back to the BEC**
  - Bragg diffraction
  - Spinor condensates
  - Collective oscillations
  - Optical lattices



# Absorption Imaging



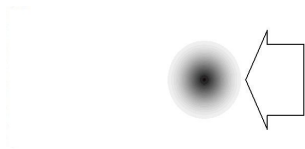
## Absorption

is the most prevalent diagnostic, unrivalled in its combination of simplicity and high signal to noise.

The number of atoms, the temperature and the density at each stage of the experiment can be detected by the absorption imaging.



# Absorption Imaging - idea

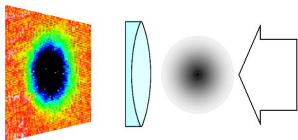


The short pulse

of the resonant laser light is fired into the cloud of atoms.



# Absorption Imaging - idea



The short pulse

of the resonant laser light is fired into the cloud of atoms.

The cloud of atoms cast the absorption shadow on the CCD camera.



# Absorption Imaging - pros and cons

- Is pretty simple
- High signal-to-noise ratio
- Brings plenty of information
- CCD cameras are slow
- Absorption imaging is destructive
- *In situ* imaging is hard or impossible
- Needs considerable optical access



# Absorption Imaging - pros and cons

- Is pretty simple
- High signal-to-noise ratio
- Brings plenty of information
- CCD cameras are slow
- Absorption imaging is destructive
- *In situ* imaging is hard or impossible
- Needs considerable optical access



# Absorption Imaging - pros and cons

- Is pretty simple
- High signal-to-noise ratio
- Brings plenty of information
- CCD cameras are slow
- Absorption imaging is destructive
- *In situ* imaging is hard or impossible
- Needs considerable optical access



# Absorption Imaging - pros and cons

- Is pretty simple
- High signal-to-noise ratio
- Brings plenty of information
- CCD cameras are slow
- Absorption imaging is destructive
- *In situ* imaging is hard or impossible
- Needs considerable optical access





# Absorption Imaging - pros and cons

- Is pretty simple
- High signal-to-noise ratio
- Brings plenty of information
- CCD cameras are slow
- Absorption imaging is destructive
- *In situ* imaging is hard or impossible
- Needs considerable optical access



# Absorption Imaging - pros and cons

- Is pretty simple
- High signal-to-noise ratio
- Brings plenty of information
- CCD cameras are slow
- Absorption imaging is destructive
- *In situ* imaging is hard or impossible
- Needs considerable optical access

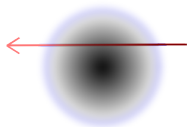


# Absorption Imaging - pros and cons

- Is pretty simple
- High signal-to-noise ratio
- Brings plenty of information
- CCD cameras are slow
- Absorption imaging is destructive
- *In situ* imaging is hard or impossible
- Needs considerable optical access



## Absorption Imaging - image analysis



Index of refraction of a dilute atomic vapor  $n_{ref}$

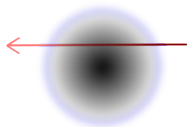
is directly related to the atomic density as

$$n_{ref} = 1 + \frac{\sigma_0 n \lambda}{4\pi} \left[ \frac{i}{1 + \sigma^2} - \frac{\sigma}{1 + \sigma^2} \right] \quad (1)$$

$\sigma_0$  is the resonant cross-section,  $\lambda$  is the wavelength of the probe light, and  $\sigma = \frac{\omega - \omega_0}{\Gamma/2}$  is the detuning of the probe light from the atomic resonance frequency in half-line widths.



# Absorption Imaging - image analysis



Index of refraction of a dilute atomic vapor  $n_{ref}$

is directly related to the atomic density as

$$n_{ref} = 1 + \frac{\sigma_0 n \lambda}{4\pi} \left[ \frac{i}{1 + \sigma^2} - \frac{\sigma}{1 + \sigma^2} \right] \quad (1)$$

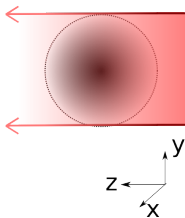
$\sigma_0$  is the resonant cross-section,  $\lambda$  is the wavelength of the probe light, and  $\sigma = \frac{\omega - \omega_0}{\Gamma/2}$  is the detuning of the probe light from the atomic resonance frequency in half-line widths.

## Multilevel atom

The index of refraction arises from several resonances and will be generally polarisation dependent.



# Absorption Imaging - image analysis



## An atomic sample

is illuminated uniformly by light propagating in the  $z$  direction. The complex electric field  $\vec{E}(x, y)$  of the probe light after passage through the atomic sample is changed from  $\vec{E}_0$  to

$$\vec{E}(x, y) = \vec{E}_0 \exp\left(-\frac{2\pi i}{\lambda} \int [n_{ref} - 1] dz\right) \quad (2)$$

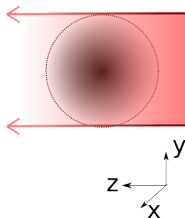
$$= t \vec{E}_0 e^{i\phi} \quad (3)$$

$t$  is the transmission and  $\phi$  is the phase shift, both depend on the product of the column density  $\tilde{n} = \int n dz$  and  $\sigma_0$ .



# Absorption Imaging - image analysis

$t$  is the transmission and  $\phi$  is the phase shift, both depend on the product of the column density  $\tilde{n} = \int n dz$  and  $\sigma_0$ .



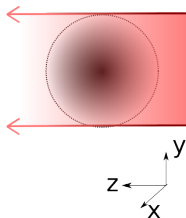
$$t = \exp\left(-\frac{\tilde{n}\sigma_0}{2} \frac{1}{1+\delta^2}\right) = e^{\tilde{D}/2} \quad (4)$$

$$\phi = -\frac{\tilde{n}\sigma_0}{2} \frac{\delta}{1+\delta^2} = -\delta \frac{\tilde{D}}{2} \quad (5)$$



# Absorption Imaging - image analysis

$t$  is the transmission and  $\phi$  is the phase shift, both depend on the product of the column density  $\tilde{n} = \int n dz$  and  $\sigma_0$ .



$$t = \exp\left(-\frac{\tilde{n}\sigma_0}{2} \frac{1}{1+\delta^2}\right) = e^{\tilde{D}/2} \quad (4)$$

$$\phi = -\frac{\tilde{n}\sigma_0}{2} \frac{\delta}{1+\delta^2} = -\delta \frac{\tilde{D}}{2} \quad (5)$$

where

$$\tilde{D}(x, y) = \frac{\sigma_0}{1+\delta^2} \int n(x, y, z) dz = \frac{\tilde{n}\sigma_0}{1+\delta^2} \quad (6)$$

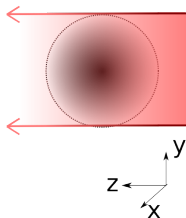
is the off-resonance **optical density**





## Absorption Imaging - image analysis

$t$  is the transmission and  $\phi$  is the phase shift, both depend on the product of the column density  $\tilde{n} = \int n dz$  and  $\sigma_0$ .



$$t = \exp\left(-\frac{\tilde{n}\sigma_0}{2} \frac{1}{1+\delta^2}\right) = e^{\tilde{D}/2} \quad (4)$$

$$\phi = -\frac{\tilde{n}\sigma_0}{2} \frac{\delta}{1+\delta^2} = -\delta \frac{\tilde{D}}{2} \quad (5)$$

where

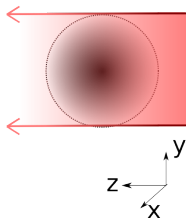
$$\tilde{D}(x, y) = \frac{\sigma_0}{1+\delta^2} \int n(x, y, z) dz = \frac{\tilde{n}\sigma_0}{1+\delta^2} \quad (6)$$

is the off-resonance **optical density**

Because CCD camera photosensors aren't sensitive to phase, the absorption image shows the spatial variation of  $t^2$ . Thus  $\tilde{D}(x, y) = -\ln t^2$



## Absorption Imaging - image analysis

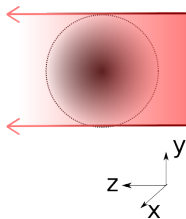

 $t^2 \mapsto \text{Intensity } I$ 

The change of intensity  $I$  in the **resonant** probe laser beam during propagation through the sample in the  $z$  direction can be described as

$$\frac{dI}{dz} = -I n \sigma_0 \quad (7)$$



## Absorption Imaging - image analysis


 $t^2 \mapsto \text{Intensity } I$ 

The change of intensity  $I$  in the **resonant** probe laser beam during propagation through the sample in the  $z$  direction can be described as

$$\frac{dI}{dz} = -I n \sigma_0 \quad (7)$$

For a two-level atom, the cross-section is given by  $\sigma_0 = \frac{3}{2} \frac{\lambda^2}{\pi}$

Solving Eq. (7) yields

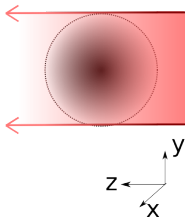
$$\ln \left( \frac{I_f}{I_i} \right) = -\sigma_0 \tilde{n}(x, y) \quad (8)$$

where  $I_i$  and  $I_f$  are the intensities before and after the sample



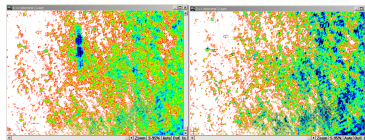
## Absorption Imaging - image analysis

Solving Eq. (7) yields  $\ln\left(\frac{I_f}{I_i}\right) = -\sigma_0 \tilde{n}(x, y)$ .

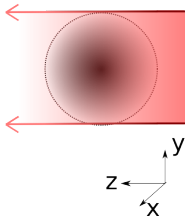


CCD camera

$I_f$  corresponds to the picture taken with the cloud,  
 $I_i$  corresponds to the picture taken without the cloud

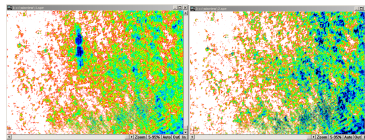


## Absorption Imaging - image analysis

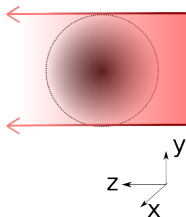


CCD camera

$I_f$  corresponds to the picture taken with the cloud,  
 $I_i$  corresponds to the picture taken without the cloud  
 $I_d$ , the dark field picture has to be subtracted from both  $I_f$  and  $I$



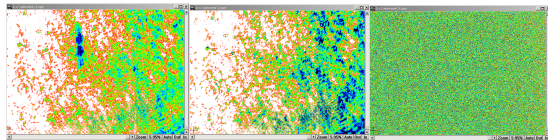
## Absorption Imaging - image analysis



CCD camera

$I_f$  corresponds to the picture taken with the cloud,  
 $I_i$  corresponds to the picture taken without the cloud  
 $I_d$ , the dark field picture has to be subtracted from both  $I_f$  and  $I_i$

$$\ln \left( \frac{I_f - I_d}{I_i - I_d} \right) = -\sigma_0 \tilde{n}(x, y) \quad (9)$$



INNOWACYJNA GOSPODARKA  
NARODOWA STRATEGIA SPÓJNOŚCI

UNIA EUROPEJSKA  
EUROPEJSKI FUNDUSZ  
ROZWOJU REGIONALNEGO

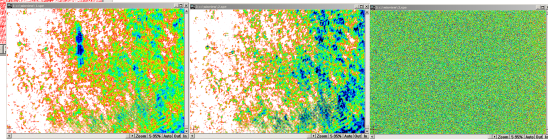
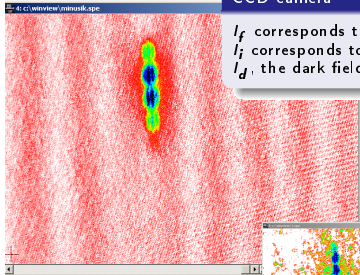


## Absorption Imaging - image analysis

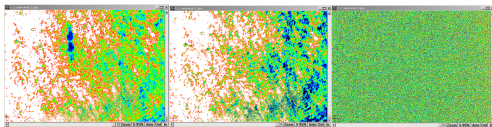
CCD camera

$I_f$  corresponds to the picture taken with the cloud,  
 $I_i$  corresponds to the picture taken without the cloud  
 $I_d$ , the dark field picture has to be subtracted from both  $I_f$  and  $I$

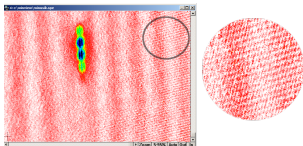
$$\ln \left( \frac{I_f - I_d}{I_i - I_d} \right) = -\sigma_0 \tilde{n}(x, y) \quad (9)$$



# Absorption Imaging - defringing



There are interference fringes on the  $I_i$  and  $I_f$  pictures. If both the picture are made under the same conditions, the fringes are the same and subtract themselves in the final image.



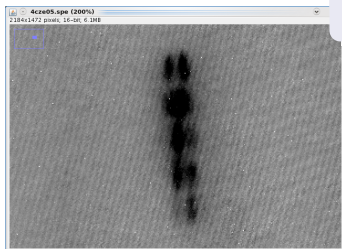
## CCD cameras

are generally slow - digitalization of 16 bits pixels takes some time. Few seconds between both pictures is more than enough for the imaging system to fluctuate a bit.





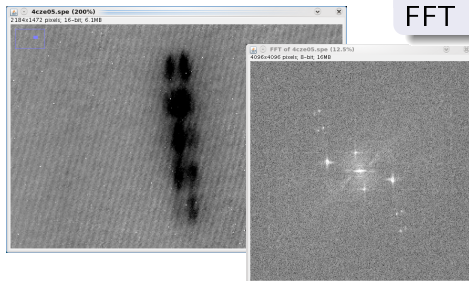
# Absorption Imaging - defringing



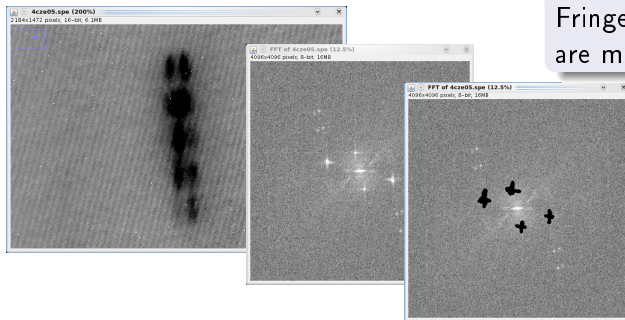
Heavily fringed image



# Absorption Imaging - defringing



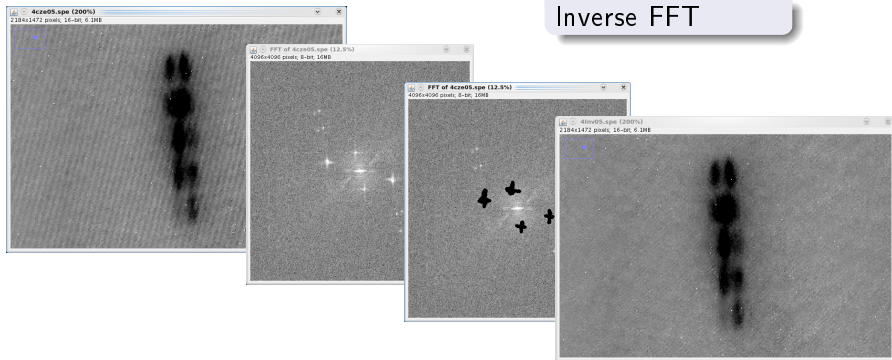
## Absorption Imaging - defringing



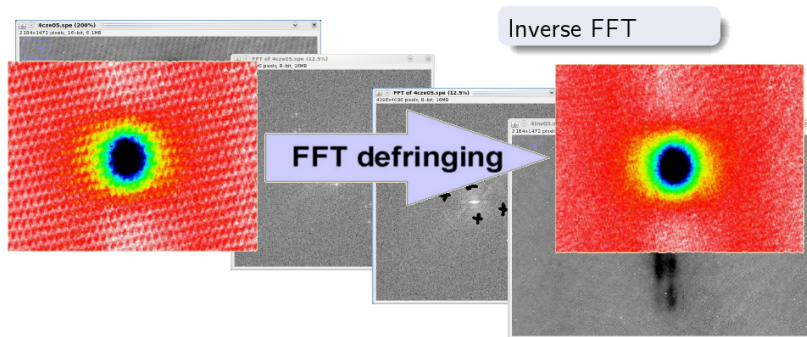
Fringes frequencies  
are masked.



# Absorption Imaging - defringing



## Absorption Imaging - defringing



# Absorption Imaging - free-fall expansion

## Why not *In situ*?

- Enormous Optical Density
- Detuning reduces OD, but produces nonlinear effects
- Condensate in the trap is very, very small
- Magnetic trap = Zeeman shifts

## Advantages of free-fall expansion

- Temperature measurement
- Spatially separate thermal and degenerate clouds



# Absorption Imaging - free-fall expansion

## Why not *In situ*?

- **Enormous Optical Density**
- Detuning reduces OD, but produces nonlinear effects
- Condensate in the trap is very, very small
- Magnetic trap = Zeeman shifts

## Advantages of free-fall expansion

- Temperature measurement
- Spatially separate thermal and degenerate clouds



# Absorption Imaging - free-fall expansion

## Why not *In situ*?

- Enormous Optical Density
- Detuning reduces OD, but produces nonlinear effects
- Condensate in the trap is very, very small
- Magnetic trap = Zeeman shifts

## Advantages of free-fall expansion

- Temperature measurement
- Spatially separate thermal and degenerate clouds





# Absorption Imaging - free-fall expansion

## Why not *In situ*?

- Enormous Optical Density
- Detuning reduces OD, but produces nonlinear effects
- Condensate in the trap is very, very small
- Magnetic trap = Zeeman shifts

## Advantages of free-fall expansion

- Temperature measurement
- Spatially separate thermal and degenerate clouds



# Absorption Imaging - free-fall expansion

## Why not *In situ*?

- Enormous Optical Density
- Detuning reduces OD, but produces nonlinear effects
- Condensate in the trap is very, very small
- Magnetic trap = Zeeman shifts

## Advantages of free-fall expansion

- Temperature measurement
- Spatially separate thermal and degenerate clouds



# Absorption Imaging - free-fall expansion

## Why not *In situ*?

- Enormous Optical Density
- Detuning reduces OD, but produces nonlinear effects
- Condensate in the trap is very, very small
- Magnetic trap = Zeeman shifts

## Advantages of free-fall expansion

- Temperature measurement
- Spatially separate thermal and degenerate clouds



# Absorption Imaging - free-fall expansion

## Why not *In situ*?

- Enormous Optical Density
- Detuning reduces OD, but produces nonlinear effects
- Condensate in the trap is very, very small
- Magnetic trap = Zeeman shifts

## Advantages of free-fall expansion

- Temperature measurement
- Spatially separate thermal and degenerate clouds



# Absorption Imaging - free-fall expansion

## Why not *In situ*?

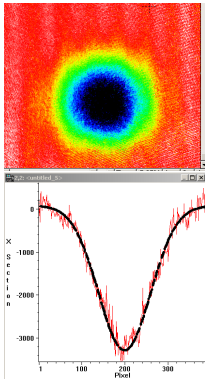
- Enormous Optical Density
- Detuning reduces OD, but produces nonlinear effects
- Condensate in the trap is very, very small
- Magnetic trap = Zeeman shifts

## Advantages of free-fall expansion

- Temperature measurement
- Spatially separate thermal and degenerate clouds



# Absorption Imaging - cold atoms



Well above the critical temperature,

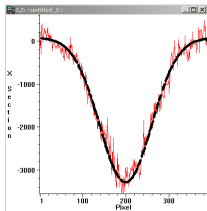
the density distribution in the thermal cloud can be described with the classical Boltzmann distribution. The column optical density is described then by the Gaussian function

$$OD_{Gauss}(x, y) = OD_{Gpeak} \exp \left[ -\frac{1}{2} \left( \frac{x - x_c}{\sigma_x} \right)^2 - \frac{1}{2} \left( \frac{y - y_c}{\sigma_y} \right)^2 \right] \quad (10)$$

with  $\sigma_x, \sigma_y$  being the half-width of the atomic density distribution,  $OD_{Gpeak}$  denotes the maximum value of the density, and  $(x_c, y_c)$  are spatial coordinates of the maximum.



# Absorption Imaging - cold atoms



Well above the critical temperature,

the density distribution in the thermal cloud can be described with the classical Boltzmann distribution. The column optical density is described then by the Gaussian function

$$OD_{\text{Gauss}}(x, y) = OD_{\text{Gpeak}} \exp \left[ -\frac{1}{2} \left( \frac{x - x_c}{\sigma_x} \right)^2 - \frac{1}{2} \left( \frac{y - y_c}{\sigma_y} \right)^2 \right] \quad (10)$$

with  $\sigma_x, \sigma_y$  being the half-width of the atomic density distribution,  $OD_{\text{Gpeak}}$  denotes the maximum value of the density, and  $(x_c, y_c)$  are spatial coordinates of the maximum.

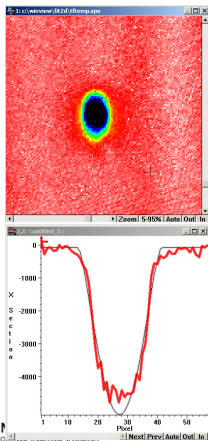
By fitting the function (10) to the data, number of atoms  $N_{th} = (2\pi)^{3/2} \frac{OD_{\text{Gpeak}}}{\sigma_0} \sigma_x^2(t) \sigma_y(t)$

and the initial atomic temperature  $T = \frac{2\tau_r^2}{1+3\tau_z^2} T_r + \frac{1+\tau_z^2}{1+3\tau_r^2} T_z$  can be determined

(where  $T_i = (m/2k_B) \left[ \omega_i^2 \sigma_i^2(t) / (1 + \tau_i^2) \right]$ , trap is cigar-shape and  $\tau_i = \omega_i t$  for  $i = x, y$ ).



# Absorption Imaging - BEC



Well below the critical temperature,

when the BEC is pure and contains big enough number of atoms, the density distribution can be described with the Thomas-Fermi distribution. The column optical density is described by the TF profile, a clipped parabola

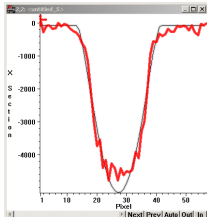
$$OD_{TF}(x, y) = OD_{TFpeak} \max \left[ 0, \left( 1 - \left( \frac{x - x_c}{R_x} \right)^2 - \left( \frac{y - y_c}{R_y} \right)^2 \right)^{3/2} \right], \quad (11)$$

where  $R_x, R_y$  are the TF radii and  $OD_{TFpeak}$  denotes maximum of the condensate optical density.





# Absorption Imaging - BEC



Well below the critical temperature,

when the BEC is pure and contains big enough number of atoms, the density distribution can be described with the Thomas-Fermi distribution. The column optical density is described by the TF profile, a clipped parabola

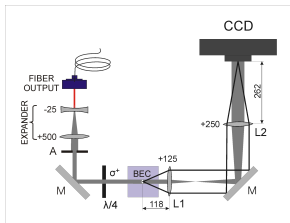
$$OD_{TF}(x, y) = OD_{TFpeak} \max \left[ 0, \left( 1 - \left( \frac{x - x_c}{R_x} \right)^2 - \left( \frac{y - y_c}{R_y} \right)^2 \right)^{3/2} \right], \quad (11)$$

where  $R_x, R_y$  are the TF radii and  $OD_{TFpeak}$  denotes maximum of the condensate optical density.

By fitting the function (11) to the data, number of atoms  $N_{BEC} = \frac{8}{15} \pi \frac{OD_{TFpeak}}{\sigma_0} R_x^2(t) R_y(t)$  can be determined.



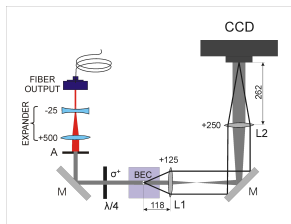
# Absorption Imaging - actual realisation



- Beam is spatially filtered by a single-mode fiber
- Beam is expanded by a telescope
- A diaphragm selects the small, central, most intense and uniform area
- Beam is circularly polarised and a low magnetic field is applied
- The absorption shadow of the sample is imaged through a telescope onto the CCD camera



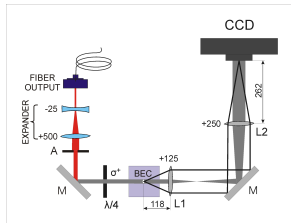
# Absorption Imaging - actual realisation



- Beam is spatially filtered by a single-mode fiber
- Beam is expanded by a telescope
- A diaphragm selects the small, central, most intense and uniform area
- Beam is circularly polarised and a low magnetic field is applied
- The absorption shadow of the sample is imaged through a telescope onto the CCD camera



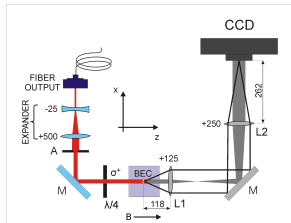
# Absorption Imaging - actual realisation



- Beam is spatially filtered by a single-mode fiber
- Beam is expanded by a telescope
- A diaphragm selects the small, central, most intense and uniform area
- Beam is circularly polarised and a low magnetic field is applied
- The absorption shadow of the sample is imaged through a telescope onto the CCD camera



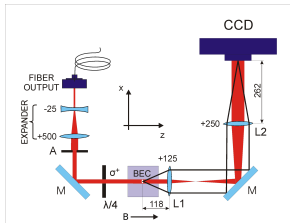
# Absorption Imaging - actual realisation



- Beam is spatially filtered by a single-mode fiber
- Beam is expanded by a telescope
- A diaphragm selects the small, central, most intense and uniform area
- Beam is circularly polarised and a low magnetic field is applied
- The absorption shadow of the sample is imaged through a telescope onto the CCD camera



# Absorption Imaging - actual realisation



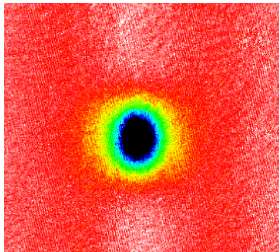
- Beam is spatially filtered by a single-mode fiber
- Beam is expanded by a telescope
- A diaphragm selects the small, central, most intense and uniform area
- Beam is circularly polarised and a low magnetic field is applied
- The absorption shadow of the sample is imaged through a telescope onto the CCD camera

# Absorption Imaging - finite temperature BEC

At finite temperatures,

the BEC fraction is always associated with some fraction of thermal (noncondensed) atoms.

Each of the fractions has different density distribution and contributes differently to the recorded image.

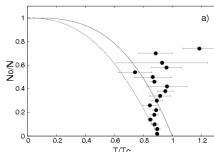


# Absorption Imaging - finite temperature BEC

At finite temperatures,

the BEC fraction is always associated with some fraction of thermal (noncondensed) atoms.

Each of the fractions has different density distribution and contributes differently to the recorded image.

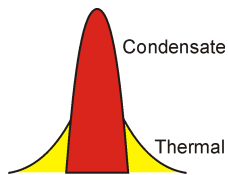


A simplistic analysis of such bimodal distributions by fitting them to a sum of the Gaussian and Thomas-Fermi functions corresponding to the thermal and condensate fractions, respectively, is not satisfactory and leads to systematic errors.





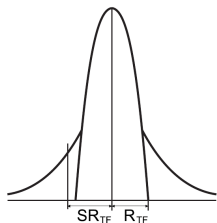
# Absorption Imaging - finite temperature BEC



- The temperature is determined from the wings of the thermal distribution
- It is hard to tell where the degenerate region is and where is not
- Close to the  $T_C$ , thermal distribution is no longer the Gaussian but the so-called Bose-Enhanced Gaussian



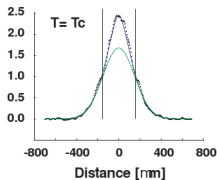
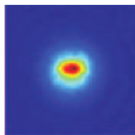
# Absorption Imaging - finite temperature BEC



- The temperature is determined from the wings of the thermal distribution
- It is hard to tell where the degenerate region is and where is not
- Close to the  $T_C$ , thermal distribution is no longer the Gaussian but the so-called Bose-Enhanced Gaussian



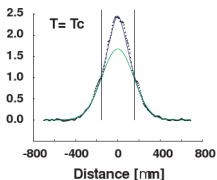
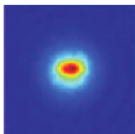
# Absorption Imaging - finite temperature BEC



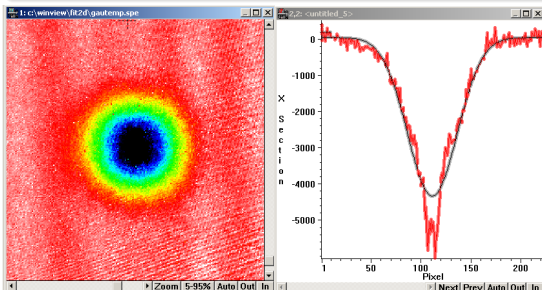
- The temperature is determined from the wings of the thermal distribution
- It is hard to tell where the degenerate region is and where is not
- Close to the  $T_C$ , thermal distribution is no longer the Gaussian but the so-called Bose-Enhanced Gaussian



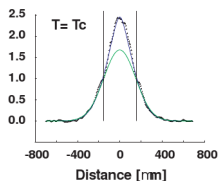
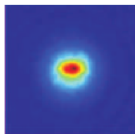
# Absorption Imaging - finite temperature BEC



Close to the  $T_C$ , thermal distribution is no longer the Gaussian but the so-called Bose-Enhanced Gaussian (with chemical potential set to zero):



## Absorption Imaging - finite temperature BEC



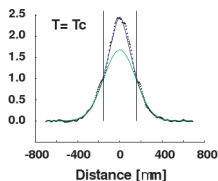
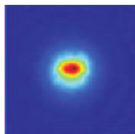
Close to the  $T_C$ , thermal distribution is no longer the Gaussian but the so-called Bose-Enhanced Gaussian (with chemical potential set to zero):

$$OD_{EnhGauss}(x, y) = OD_{Gpeak} \frac{g_2 \left[ \exp \left[ -\frac{1}{2} \left( \frac{x-x_c}{\sigma_x} \right)^2 - \frac{1}{2} \left( \frac{y-y_c}{\sigma_y} \right)^2 \right] \right]}{g_2(1)}, \quad (12)$$

where  $g_2(x) = \sum_{n=1}^{\infty} (x^n) / (n^2)$  (see, e.g. K. Huang, *Statistical Mechanics*).



# Absorption Imaging - finite temperature BEC



Close to the  $T_C$ , thermal distribution is no longer the Gaussian but the so-called Bose-Enhanced Gaussian (with chemical potential set to zero):

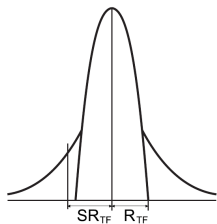
$$OD_{EnhGauss}(x, y) = OD_{Gpeak} \frac{g_2 \left[ \exp \left[ -\frac{1}{2} \left( \frac{x-x_c}{\sigma_x} \right)^2 - \frac{1}{2} \left( \frac{y-y_c}{\sigma_y} \right)^2 \right] \right]}{g_2(1)}, \quad (12)$$

where  $g_2(x) = \sum_{n=1}^{\infty} (x^n) / (n^2)$  (see, e.g. K. Huang, *Statistical Mechanics*).

With an increase of the distance from the position of maximum density, the series terms in numerator of (12) decrease to zero. At appropriate distance, function (12) becomes the Gauss function (10) which justifies description of the density distribution at edges of the thermal fraction by function (10). Nevertheless, more accurate results are obtained if the first three terms of the series (12) are used instead. Higher terms do not improve meaningfully the accuracy but they increase consumption of the computational power.



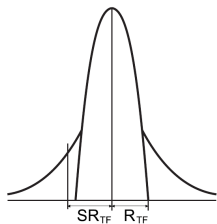
# Absorption Imaging - finite temperature BEC



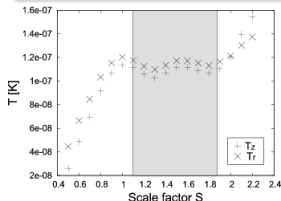
It is hard to tell where the degenerate region is and where is not



## Absorption Imaging - finite temperature BEC

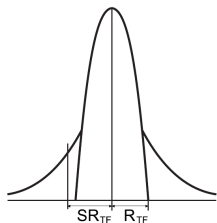


It is hard to tell where the degenerate region is and where is not

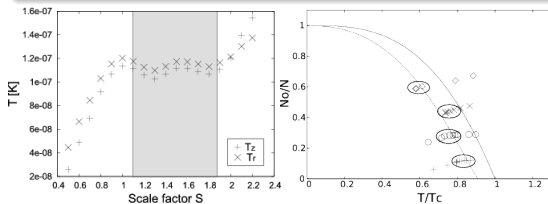




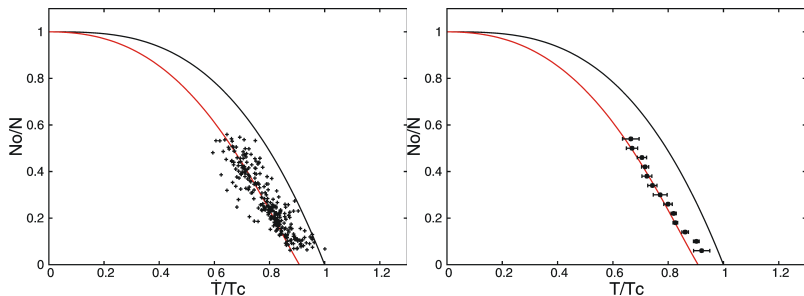
## Absorption Imaging - finite temperature BEC



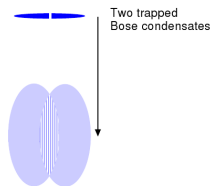
It is hard to tell where the degenerate region is and where is not



# Absorption Imaging - finite temperature BEC



# Absorption Imaging - condensate interferometry



- Two BECs expand freely and overlap
- Do they interfere? - **YES!**
- Is the interference pattern stable in time and space? - **NO!**
- If not, how can we see it?

## Detection

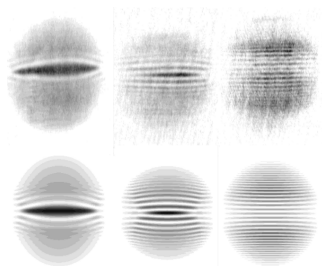
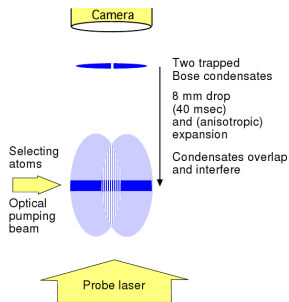


INNOWACYJNA GOSPODARKA  
NARODOWA STRATEGIA SPÓJNOŚCI

UNIA EUROPEJSKA  
EUROPEJSKI FUNDUSZ  
ROZWOJU REGIONALNEGO



# Absorption Imaging - condensate interferometry



## Detection

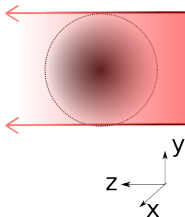
INNOWACYJNA GOSPODARKA  
NARODOWA STRATEGIA SPÓJNOŚCI

UNIA EUROPEJSKA  
EUROPEJSKI FUNDUSZ  
ROZWOJU REGIONALNEGO



# Phase-contrast

$t$  is the transmission and  $\phi$  is the phase shift, both depend on the product of the column density  $\tilde{n} = \int n dz$  and  $\sigma_0$ .



$$t = \exp\left(-\frac{\tilde{n}\sigma_0}{2} \frac{1}{1+\delta^2}\right) = e^{\tilde{D}/2} \quad (13)$$

$$\phi = -\frac{\tilde{n}\sigma_0}{2} \frac{\delta}{1+\delta^2} = -\delta \frac{\tilde{D}}{2} \quad (14)$$

where

$$\tilde{D}(x, y) = \frac{\sigma_0}{1+\delta^2} \int n(x, y, z) dz = \frac{\tilde{n}\sigma_0}{1+\delta^2} \quad (15)$$

is the off-resonance **optical density**

Optical Density can be determined also by phase measurements. **But how can we measure the phase?**



# Phase-contrast

Absorption imaging is done by illuminating the atoms with a laser beam and imaging the shadow cast by the atoms onto a CCD camera. Because photosensors aren't sensitive to phase, the absorption image shows the spatial variation of  $t^2$

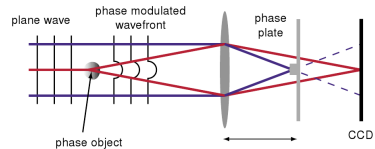
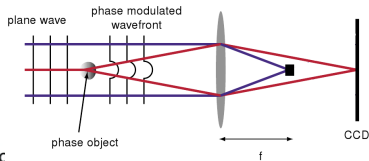
To image a transparent object, information encoded in the phase shift of the light must be converted into intensity information which can be detected by a photosensor.



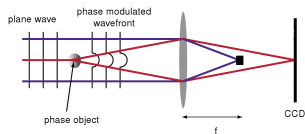
# Phase-contrast

Absorption imaging is done by illuminating the atoms with a laser beam and imaging the shadow cast by the atoms onto a CCD camera. Because photosensors aren't sensitive to phase, the absorption image shows the spatial variation of  $t^2$

To image a transparent object, information encoded in the phase shift of the light must be converted into intensity information which can be detected by a photosensor.



# Phase-contrast - Dark Ground imaging

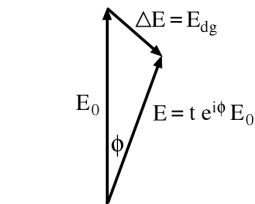


The simplest form of spatial filtering is to **block the unscattered light** by placing a small opaque object into the Fourier plane

The probe light field after passing through the atoms can be separated into the scattered and unscattered radiation

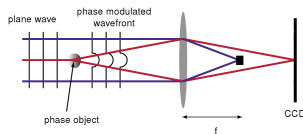
$$E = tE_0 e^{i\phi} = E_0 + \Delta E \quad (16)$$

Blocking the unscattered light gives the dark-ground signal





# Phase-contrast - Dark Ground imaging



The simplest form of spatial filtering is to **block the unscattered light** by placing a small opaque object into the Fourier plane

The probe light field after passing through the atoms can be separated into the scattered and unscattered radiation

$$E = tE_0 e^{i\phi} = E_0 + \Delta E \quad (16)$$

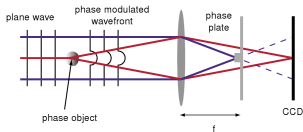
Blocking the unscattered light gives the dark-ground signal

$$\langle I_{dg} \rangle = \frac{1}{2} |E - E_0|^2 = I_0 [1 + t^2 - 2t \cos \phi] \quad (17)$$

For small  $\phi$  the dark-ground signal is quadratic in  $\phi$ .

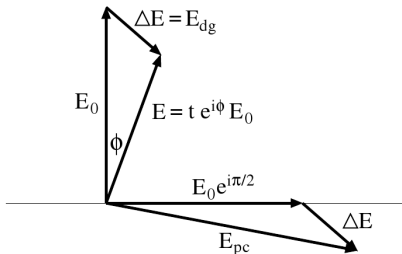


# Phase-contrast - Phase Contrast imaging

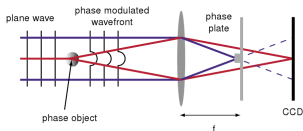


Phase-contrast imaging is accomplished by **shifting the phase** of the unscattered light by  $\pm\pi/2$  in the Fourier plane of the imaging lens

This is done with a "phase plate" which is an optical flat with a small bump or dimple in the centre.



# Phase-contrast - Phase Contrast imaging



Phase-contrast imaging is accomplished by **shifting the phase** of the unscattered light by  $\pm\pi/2$  in the Fourier plane of the imaging lens

This is done with a "phase plate" which is an optical flat with a small bump or dimple in the centre.

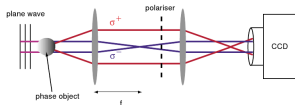
The intensity of a point in the image plane is then

$$\langle I_{pc} \rangle = \frac{1}{2} |E + E_0 (e^{\pm i \frac{\pi}{2}} - 1)|^2 = I_0 \left[ 2 + t^2 - 2\sqrt{2}t \cos \left( \phi \pm \frac{\pi}{4} \right) \right] \quad (18)$$

For small  $\phi$  one obtains  $\langle I_{pc} \rangle \simeq I_0 [t^2 + 2 - 2t \pm 2t\phi]$



# Phase-contrast - Polarisation Contrast imaging



Linearly polarised light with both  $\sigma^-$  and  $\sigma^+$

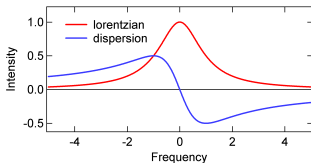
components is incident on the condensate. In the presence of **high magnetic fields**, the degeneracy of the transitions excited by these components is lifted, and the detuning can be chosen so that only one component interacts with a transition.

In the diagram, this is the  $\sigma^+$  component. The polariser is rotated to either **block out** the unscattered light, or to cause the two polarisations to **interfere**.

This method is not universally applicable. *E.g.* the standard imaging geometry for a Ioffe-Pritchard trap involves a probe beam propagating perpendicular to the axis of a **low** magnetic bias field.



# Phase-contrast - Non-destructive measurements

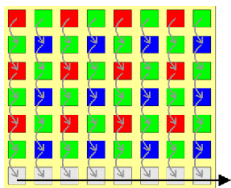
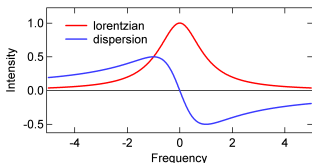


Optical detection of the condensate causes heating through photon absorption and spontaneous emission

- Phase-contrast imaging is indeed less destructive than an absorptive technique for an optically thick cloud such as a BEC.
- Using phase-contrast, multiple images of the same condensate can be taken.
- There is a catch. Phase contrast imaging is slow, because in its current incarnation, it relies on a CCD camera.



# Phase-contrast - Non-destructive measurements

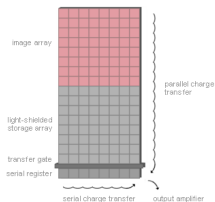
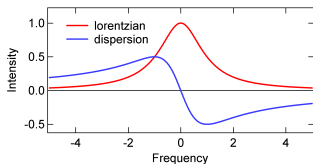


Optical detection of the condensate causes heating through photon absorption and spontaneous emission

- Phase-contrast imaging is indeed less destructive than an absorptive technique for an optically thick cloud such as a BEC.
- Using phase-contrast, multiple images of the same condensate can be taken.
- There is a catch. Phase contrast imaging is slow, because in its current incarnation, it relies on a CCD camera.



# Phase-contrast - Non-destructive measurements



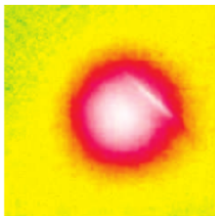
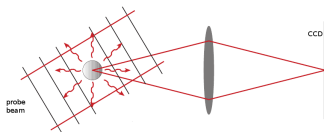
Optical detection of the condensate causes heating through photon absorption and spontaneous emission

- Phase-contrast imaging is indeed less destructive than an absorptive technique for an optically thick cloud such as a BEC.
- Using phase-contrast, multiple images of the same condensate can be taken.
- There is a catch. Phase contrast imaging is slow, because in its current incarnation, it relies on a CCD camera.

Even utilizing frame-transfer, which can take sequential pictures at rates of kHz, only a maximum of approximately 20 images can be stored, and the time lag to downloading the data for feedback is on the order of seconds with the current technology.



# Fluorescence



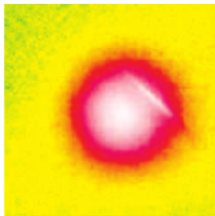
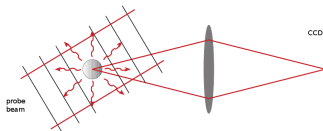
Fluorescence is a technique that has several advantages over absorption

- It does not require optical access right through the glass cell
- Absence of interference fringes





# Fluorescence



Fluorescence is a technique that has several advantages over absorption

- It does not require optical access right through the glass cell
- Absence of interference fringes

But

- It not self-calibrating
- In optically thick samples, only the fluorescence from the outer shell of the cloud will reach the camera without reabsorption.

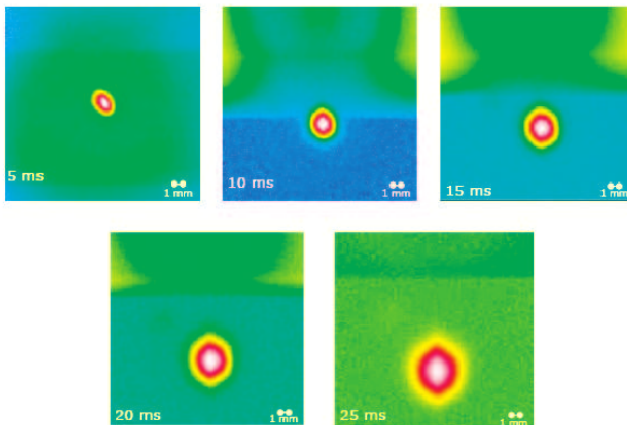


INNOWACYJNA GOSPODARKA  
NARODOWA STRATEGIA SPÓJNOŚCI

UNIA EUROPEJSKA  
EUROPEJSKI FUNDUSZ  
ROZWOJU REGIONALNEGO



# Fluorescence - temperature measurement

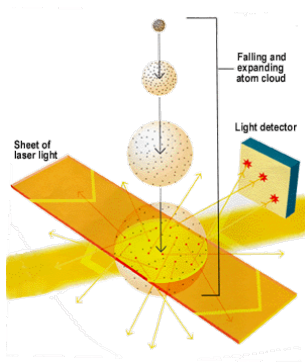


# Outline

- 1 Imaging
  - Absorption imaging
  - Phase-contrast and polarisation-contrast imaging
  - Fluorescence
- 2 Small beam techniques
  - Time of flight
  - Pump-probe spectroscopy in an operating trap
  - FWM
- 3 No beam at all
  - Release and recapture
  - Parametric resonance
  - Studies of the cold atoms collisions
- 4 Back to the BEC
  - Bragg diffraction
  - Spinor condensates
  - Collective oscillations
  - Optical lattices

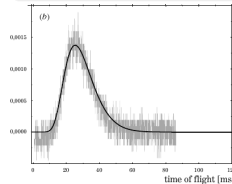


# Time of flight



## The so-called time-of-flight (TOF)

measurements are performed either by acquiring the absorption signal of the probe laser beam through the falling and expanding atomic cloud, or by measuring the fluorescence of the atoms excited by the resonant probe light.



# Time of flight

Maxwell distribution gives  $\exp\left(-\frac{v^2}{2\langle v^2 \rangle}\right) = \exp\left(-\frac{mv^2}{2k_B T}\right)$   
thus the temperature in a MOT  $T = \frac{m}{k_B} \langle v^2 \rangle$



# Time of flight

Maxwell distribution gives  $\exp\left(-\frac{v^2}{2\langle v^2 \rangle}\right) = \exp\left(-\frac{mv^2}{2k_B T}\right)$

thus the temperature in a MOT  $T = \frac{m}{k_B} \langle v^2 \rangle$

Free-fall of a single atom released from the trap can be described as  $y = \frac{1}{2}gt^2 + v_0 t$



# Time of flight

Maxwell distribution gives  $\exp\left(-\frac{v^2}{2\langle v^2 \rangle}\right) = \exp\left(-\frac{mv^2}{2k_B T}\right)$

thus the temperature in a MOT  $T = \frac{m}{k_B} \langle v^2 \rangle$

Free-fall of a single atom released from the trap can be described as  $y = \frac{1}{2}gt^2 + v_0 t$

Distribution of  $v$  and  $t$  in the distance  $y$  below the trap center:  $0 = gt\Delta t + \Delta v_0 t + \langle v_0 \rangle \Delta t$

Since  $\langle v_0 \rangle = 0$  in the trap,

$$\Delta v_0 = -g\Delta t \quad (19)$$



# Time of flight

Maxwell distribution gives  $\exp\left(-\frac{v^2}{2\langle v^2 \rangle}\right) = \exp\left(-\frac{mv^2}{2k_B T}\right)$

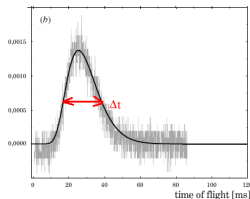
thus the temperature in a MOT  $T = \frac{m}{k_B} \langle v^2 \rangle$

Free-fall of a single atom released from the trap can be described as  $y = \frac{1}{2}gt^2 + v_0 t$

Distribution of  $v$  and  $t$  in the distance  $y$  below the trap center:  $0 = gt\Delta t + \Delta v_0 t + \langle v_0 \rangle \Delta t$

Since  $\langle v_0 \rangle = 0$  in the trap,

$$\Delta v_0 = -g\Delta t \quad (19)$$

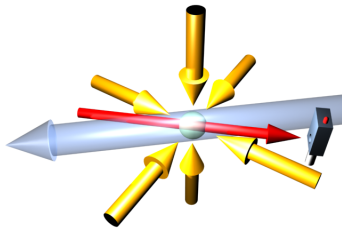


$$T = \frac{m}{k_B} (g\Delta t)^2$$





# Pump-probe spectroscopy in an operating trap

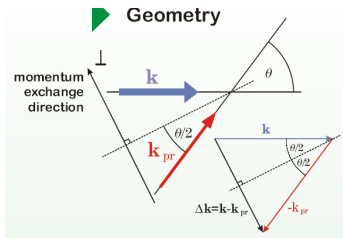


## Geometry

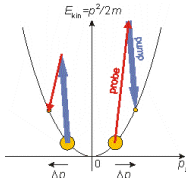
- yellow = mot beams
- blue = pump beam
- red = probe beam, frequency-scanned around the pump beam



# Recoil-Induced Resonances (RIR)

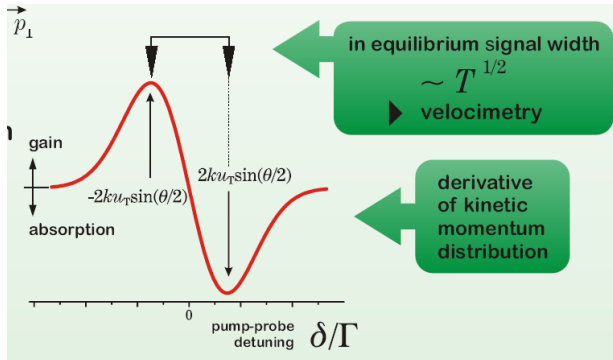


Raman transitions between the atomic momentum states. The resonance occurs whenever the probe-pump detuning coincides with the kinetic energy difference and results in atomic momentum change  $\Delta p$ .

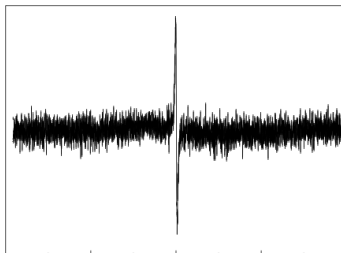
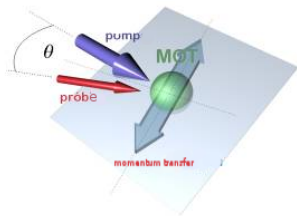


# Recoil-Induced Resonances (RIR)

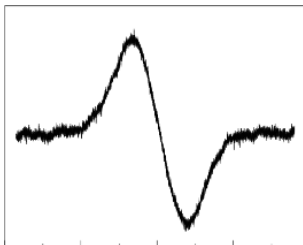
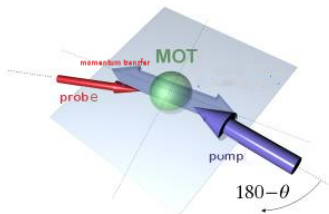
## Probe beam transmission



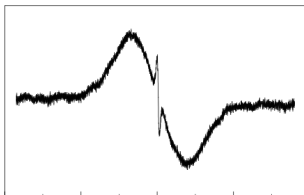
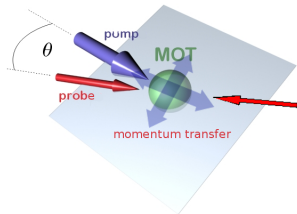
# Recoil-Induced Resonances (RIR)



# Recoil-Induced Resonances (RIR)

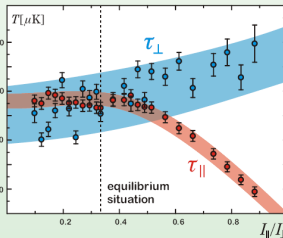
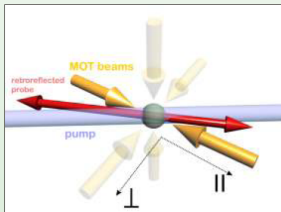


# Recoil-Induced Resonances (RIR)



# RIR + 1D MOT

uneven partition of the MOT beam intensities:



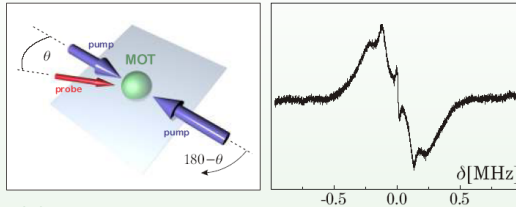
first observation of the anisotropy of momentum distribution in a MOT



# RIR + lattice

## Retroreflected pump beam

- ▶ narrow and wide RIR signal + optical lattice signal



### Advantages:

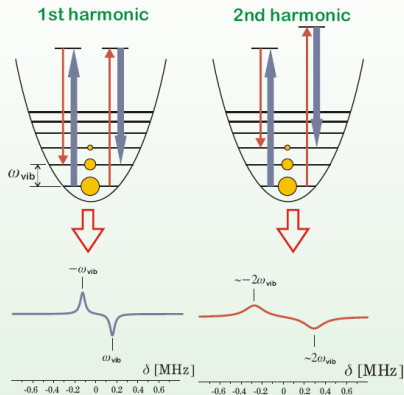
- ▶ simultaneous determination of momentum distributions in two perpendicular directions
- ▶ 1D optical lattice in a MOT  
co-existence of free and localized atoms



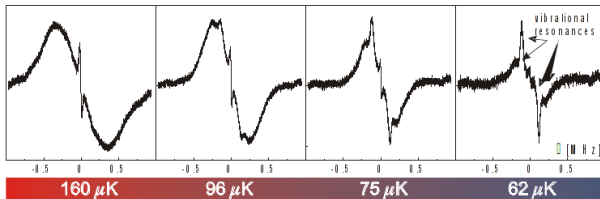


# RIR + lattice

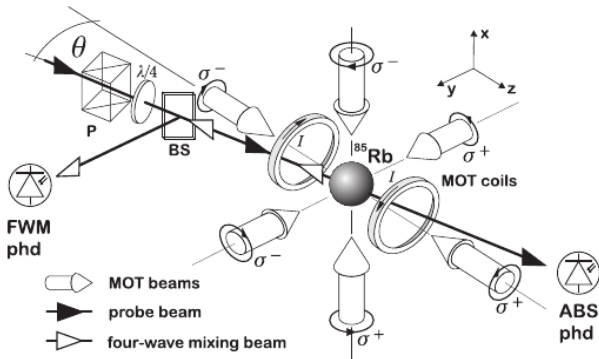
## Raman transitions between vibrational levels



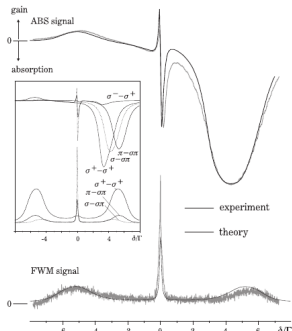
## RIR + lattice



# Four Wave Mixing (FWM)



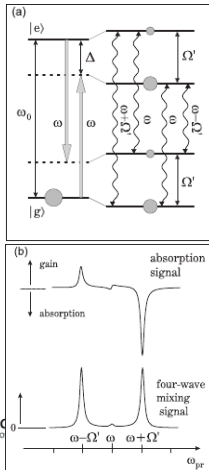
# Four Wave Mixing (FWM)



Experimental absorption (ABS) and four-wave mixing (FWM) spectra (grey lines) and their theoretical modeling (black lines).

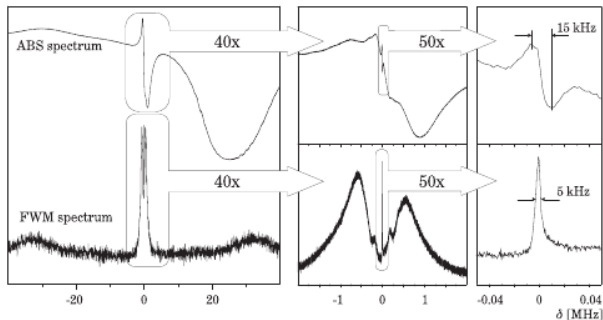


# Four Wave Mixing (FWM)



- a Two-level atom dressed by photons of monochromatic laser field of frequency  $\omega$ , red-detuned by  $\delta$  from atomic transition frequency  $\omega_0$ . Wavy arrows indicate possible transitions between dressed levels, sizes of the grey circles symbolize populations of the respective levels
- b Absorption and four-wave mixing spectra as a function of the probe beam detuning,  $\omega_{pr}$

# Four Wave Mixing (FWM)

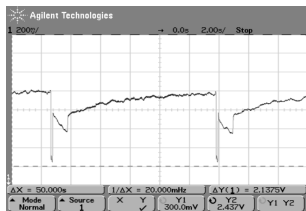


# Outline

- 1 Imaging
  - Absorption imaging
  - Phase-contrast and polarisation-contrast imaging
  - Fluorescence
- 2 Small beam techniques
  - Time of flight
  - Pump-probe spectroscopy in an operating trap
  - FWM
- 3 **No beam at all**
  - **Release and recapture**
  - **Parametric resonance**
  - **Studies of the cold atoms collisions**
- 4 Back to the BEC
  - Bragg diffraction
  - Spinor condensates
  - Collective oscillations
  - Optical lattices



# Release and recapture (RR)



Trapped cloud in a mot can be described by a thermal gas

$$dN_{gas}(v) = N_0 \exp\left(-\frac{v^2}{2\tilde{v}^2}\right) \quad (20)$$

with  $\tilde{v}^2 = \langle v^2 \rangle$  and temperature  $T = \frac{m}{k_B} \tilde{v}^2$

The atom velocity, as we already know, can be measured by releasing trapped atoms by turning off the trapping lasers and observe the time evolution of the expansion of the cloud.

Atoms are loaded into the MOT. At the time  $t = 0$  the trapping laser beams are switched off. In the dark the atomic cloud starts to expand. The trapping and slowing laser beams are turned on again at the time  $\Delta t = t_{off}$ . Atoms which remain in the trapping volume are recaptured and drift back to the trap center.





## Release and recapture (RR)

The distance,  $r(t)$ , of an atom from the trap center increases with time  $t$  as  $r(t) = vt$

The spatial distribution of the cloud of atoms is found by substituting the velocity  $v$  with the radius  $r(t)$  in Eqn. (20).

$$dN_{gas}(r) = \sqrt{\frac{2}{\pi}} \frac{r(t)^2}{t^3 \bar{v}^3} \exp\left(-\frac{r(t)^2}{2t^2 \bar{v}^2}\right) dr \quad (21)$$

The fraction,  $f(r_0; t_{off})$ , of atoms remaining within a volume of radius  $r_0$  can be obtained by integrating Eqn. (21)

$$f(r_0; t_{off}) = \int_0^{r_0} \frac{dN_{gas}(r)}{dr} d^3r \quad (22)$$



## Release and recapture (RR)

The distance,  $r(t)$ , of an atom from the trap center increases with time  $t$  as  $r(t) = vt$   
 The spatial distribution of the cloud of atoms is found by substituting the velocity  $v$  with the radius  $r(t)$  in Eqn. (20).

$$dN_{gas}(r) = \sqrt{\frac{2}{\pi}} \frac{r(t)^2}{t^3 \tilde{v}^3} \exp\left(-\frac{r(t)^2}{2t^2 \tilde{v}^2}\right) dr \quad (21)$$

The fraction,  $f(r_0; t_{off})$ , of atoms remaining within a volume of radius  $r_0$  can be obtained by integrating Eqn. (21)

$$f(r_0; t_{off}) = \int_0^{r_0} \frac{dN_{gas}(r)}{dr} d^3r = \text{erf}\left(\frac{r_0^2}{\sqrt{2} t_{off} \tilde{v}}\right) - \sqrt{\frac{2}{\pi}} \frac{r_0}{t_{off} \tilde{v}} \exp\left(-\frac{r_0^2}{2t_{off}^2 \tilde{v}^2}\right) \quad (22)$$



# Parametric resonance

With proper analysis, TOF and RR methods give very precise results. However, they are destructive as they lead to the loss of cold atomic sample. There are some nondestructive methods.

For example, one can rely on the balance between kinetic (thermal) and potential energy of atoms in the trapped gas:

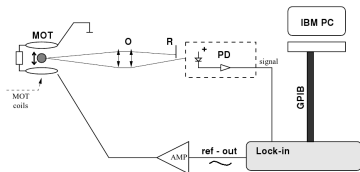
$$k_B T = k \langle x^2 \rangle$$

where  $k$  is the spring constant of the trapping potential and  $\langle x^2 \rangle$  is a mean square of the atomic position relative to the trap center.

Measuring this distance (equivalent to the cloud extension) and calculating constant  $k$  from the independent measurement of atomic oscillation in the trap, one can easily calculate the cloud temperature without switching off the trap



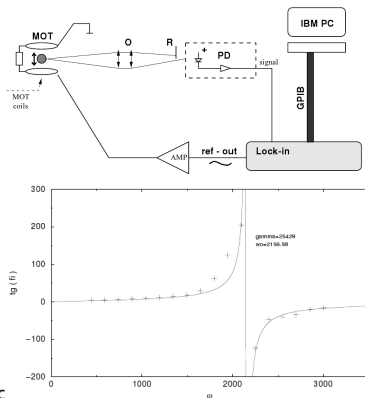
# Parametric resonance



- $k = m\omega_0^2$
- An external periodic force  $F = F_0 \cos(\omega t)$  is applied to the cloud
- The cloud can be described as 1D, driven, damped harmonic oscillator  $F = m\ddot{x} - \alpha\dot{x} - kx$
- The solution is  $x(t) = A(\omega) \cos(\omega t - \phi(\omega))$
- $\phi(\omega) = \arctan\left(\frac{\alpha\omega}{k - m\omega^2}\right) = \arctan\left(\frac{\gamma\omega}{\omega_0^2 - \omega^2}\right)$



# Parametric resonance

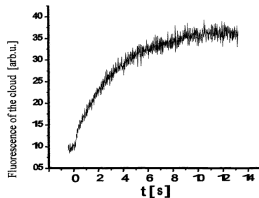


- $k = m\omega_0^2$
- An external periodic force  $F = F_0 \cos(\omega t)$  is applied to the cloud
- The cloud can be described as 1D, driven, damped harmonic oscillator  $F = m\ddot{x} - \alpha\dot{x} - kx$
- The solution is  $x(t) = A(\omega) \cos(\omega t - \phi(\omega))$
- $\phi(\omega) = \arctan\left(\frac{\alpha\omega}{k - m\omega^2}\right) = \arctan\left(\frac{\gamma\omega}{\omega_0^2 - \omega^2}\right)$



# Studies of the cold atoms collisions

When an atomic sample reaches temperatures of about 1 mK or lower, the atomic movement becomes extremely slow. In such conditions, the collisions between atoms and their corresponding interactions last much longer than in standard temperatures. It allows high sensitivity studies of very weak atomic interactions



The collision rates or cross-sections are determined by analysis of the fluorescence signal emitted by atoms during the trap loading. After the trap switch on the processes of slowing and trapping compete with the heating and escaping of atoms due to collisions. This competition is reflected onto the evolution of the number of trapped atoms  $N$ , which can be described by the following equation

$$\frac{dN}{dt} = L - \alpha N - \beta \frac{N^2}{V} \quad (23)$$

where  $L$  denotes the trap loading rate,  $V$  is its volume, and  $\alpha$  and  $\beta$  denote the rates of collisions of cold atoms with hot atom background and with other cold atoms, respectively.

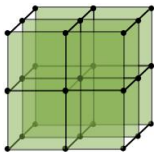


# Outline

- 1 **Imaging**
  - Absorption imaging
  - Phase-contrast and polarisation-contrast imaging
  - Fluorescence
- 2 **Small beam techniques**
  - Time of flight
  - Pump-probe spectroscopy in an operating trap
  - FWM
- 3 **No beam at all**
  - Release and recapture
  - Parametric resonance
  - Studies of the cold atoms collisions
- 4 **Back to the BEC**
  - Bragg diffraction
  - Spinor condensates
  - Collective oscillations
  - Optical lattices

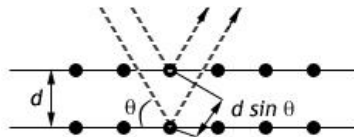
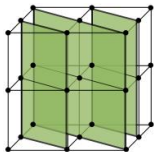


# Bragg diffraction



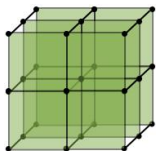
When x-rays are scattered from a crystal lattice, peaks of scattered intensity are observed which correspond to the following conditions:

- The angle of incidence = angle of scattering.
- The pathlength difference is equal to an integer number of wavelengths.



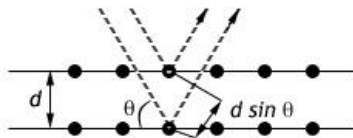
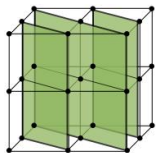


# Bragg diffraction

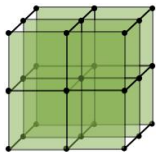


When x-rays are scattered from a crystal lattice, peaks of scattered intensity are observed which correspond to the following conditions:

- The angle of incidence = angle of scattering.
- The pathlength difference is equal to an integer number of wavelengths.

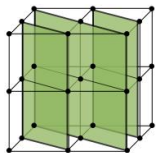


# Bragg diffraction

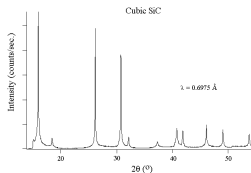


When x-rays are scattered from a crystal lattice, peaks of scattered intensity are observed which correspond to the following conditions:

- The angle of incidence = angle of scattering.
- The pathlength difference is equal to an integer number of wavelengths.



**The Bragg's law:**  $2d \sin \theta = n\lambda$

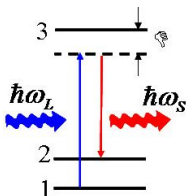


UNIA EUROPEJSKA  
EUROPEJSKI FUNDUSZ  
ROZWOJU REGIONALNEGO

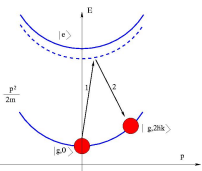


INNOWACYJNA GOSPODARKA  
NARODOWA STRATEGIA SPÓJNOŚCI

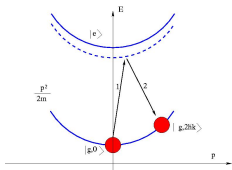
# RIR revisited



Raman transitions between the atomic momentum states. The resonance occurs whenever the probe-pump detuning coincides with the kinetic energy difference and results in atomic momentum change  $\Delta p$ .



# RIR revisited

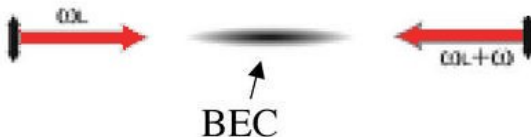


Raman transitions between the atomic momentum states. The resonance occurs whenever the probe-pump detuning coincides with the kinetic energy difference and results in atomic momentum change  $\Delta p$ .

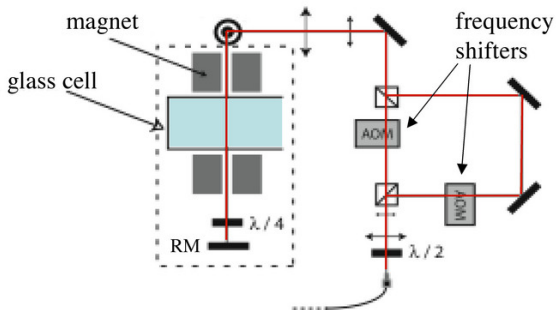
Both absorption and stimulated emission change the atomic momentum by  $\hbar k$



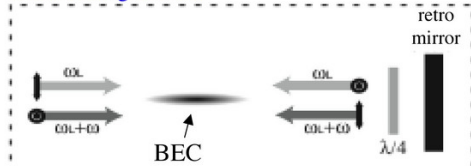
# Bragg (RIR) and BEC



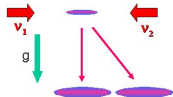
# Bragg (RIR) and BEC- experiment



## beam configuration:



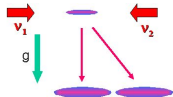
# Bragg - BEC



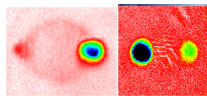
Part of the BEC is coherently moved to the other momentum state. This can be seen in the free-fall expansion.



# Bragg - BEC



Part of the BEC is coherently moved to the other momentum state. This can be seen in the free-fall expansion.

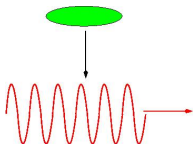


Two momentum states of the same ground state.





## Why the "Bragg scattering"?

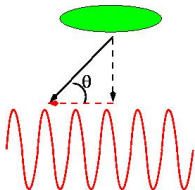
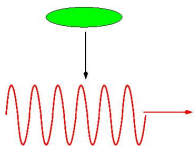


Two counter-propagating laser beams with relative detuning  $\Delta\nu$  creates a moving, optical standing wave in the laboratory frame. The velocity of the lattice is equal to  $v = \lambda\Delta\nu/2$ .

The velocity depends on  $\Delta\nu$



## Why the "Bragg scattering"?



Two counter-propagating laser beams with relative detuning  $\Delta\nu$  creates a moving, optical standing wave in the laboratory frame. The velocity of the lattice is equal to  $v = \lambda\Delta\nu/2$ .

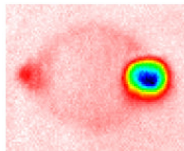
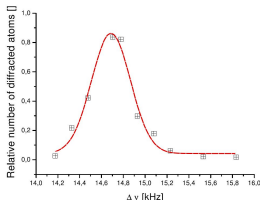
The velocity depends on  $\Delta\nu$

In a frame moving with respect to the laboratory frame, were the lattice is standing still, the condensate hits the lattice at some angle. The angle depends on  $v$ , therefore it also depends on  $\Delta\nu$



# Bragg spectroscopy

Bragg spectroscopy – dependence of the relative number in the scattered condensate on the detuning  $\Delta\nu$ .



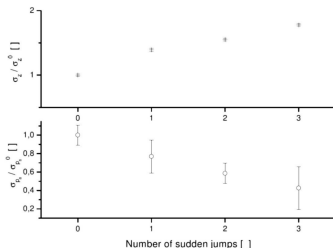
The shape of this resonance corresponds to the momentum distribution of BEC. **Direct measurement of the momentum distribution of the condensate wave function**



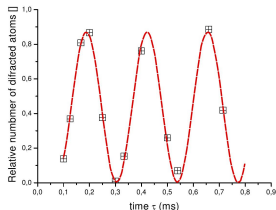
# Quadrature squeezing of the BEC

Bragg spectroscopy can be used e.g. to detect squeezed states of the condensate wave function

When the uncertainty of momentum is reduced, the uncertainty of position grows

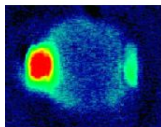


# Rabi oscillations

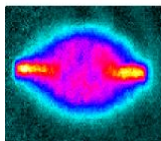


Varying the duration of the Bragg lasers pulse one can detect oscillations of the number of atoms in the scattered condensate. These oscillations are nothing else than the Rabi oscillations  $\Omega = V_{dip}/(2\hbar)$ .

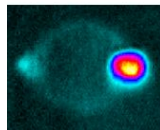
$$\Omega't < \pi/2$$



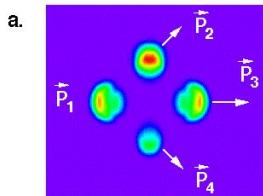
$$\Omega't = \pi/2$$



$$\Omega't \approx \pi$$

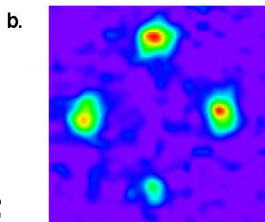


# Four wave mixing



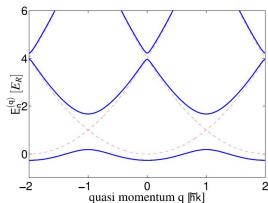
Bragg diffraction can be treated as a collision of two wave packets

$\vec{p}_1$  is the original condensate



Two perpendicular Bragg diffractions produces two scattered condensates  $\vec{p}_2$  i  $\vec{p}_4$ . Additionally, the fourth condensate appears,  $\vec{p}_3$  in the process analogous to the FWM.

# Bloch band formalism



Band structure theory originates from a study of the electron motion in a crystal lattice

In the periodic potential the atom-lattice system has an energy spectrum that exhibits a band structure

Propagation of a particle with mass  $m$  in a one dimensional periodic potential is identical to propagation of a free particle with effective mass defined as  $m^*$

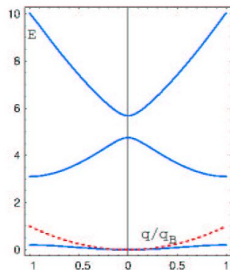
$$m_{n,q}^* = \hbar^2 \left( \frac{\partial^2 E_{n,q}}{\partial q^2} \right)^{-1}$$

and velocity in the lattice rest frame (Bloch velocity)

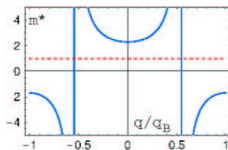
$$v_{n,q} = \frac{1}{\hbar} \frac{\partial E_{n,q}}{\partial q}$$



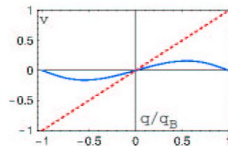
# First Brillouin zone



(a) Energy bands



(b) Effective mass

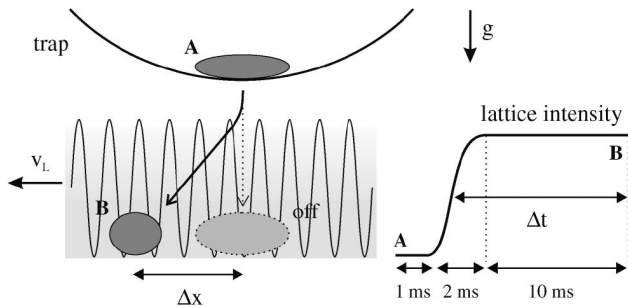


(c) Velocity





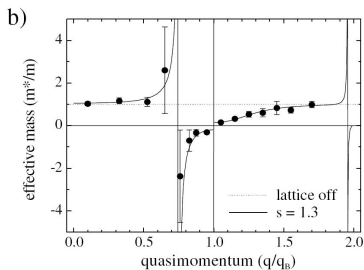
# Bloch states and a BEC



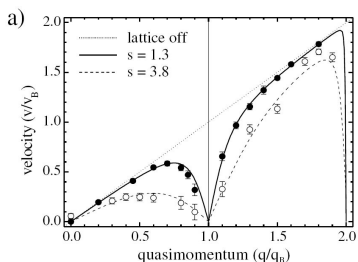
BEC is loaded into **adiabatically** switched on optical lattice



# Bloch states and a BEC - single-particle-like effects



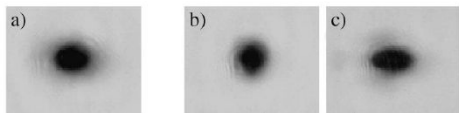
effective mass



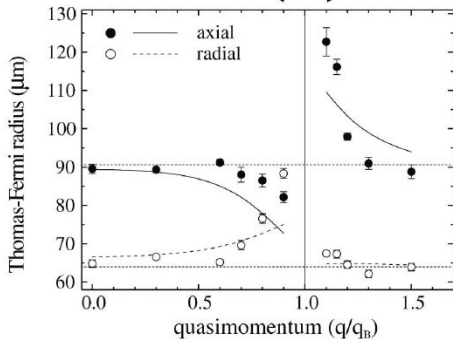
velocity in the moving lattice frame



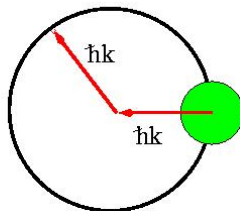
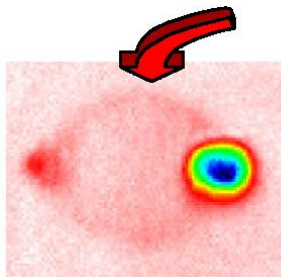
# Lensing effect on the BEC



Tuning the effective mass of the condensate allows to focus or defocus the BEC



## Two condensates collide

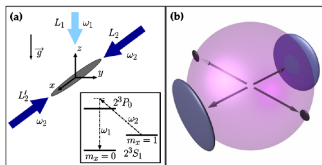


Two condensates collide - atoms in the condensates collide

Spherically symmetric s-wave scattering is the dominant type of interactions



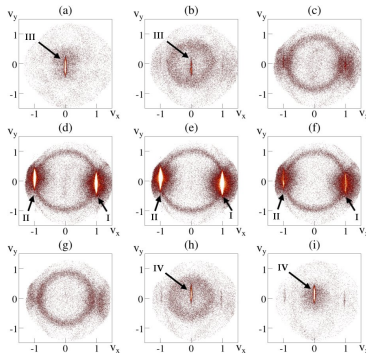
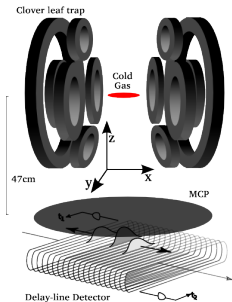
# Elastic scattering losses from colliding Bose-Einstein condensates



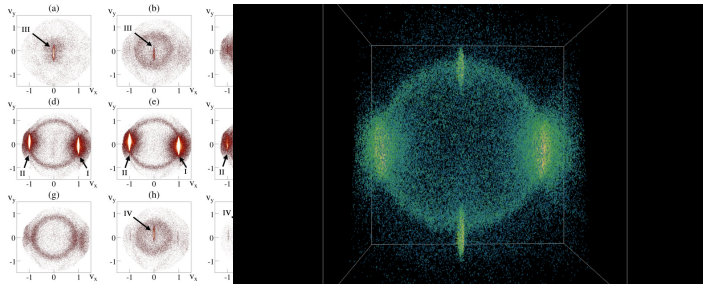
Transition from spontaneous to stimulated scattering -  
**Spontaneous Four-Wave Mixing**



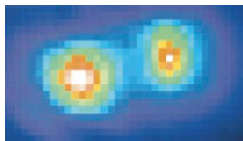
# Elastic scattering losses from colliding Bose-Einstein condensates



# Elastic scattering losses from colliding Bose-Einstein condensates



# Spinor condensates



First spinor condensates, JILA 1996  
 $F = 1, m_F = -1$  and  $F = 2, m_F = 2$





# Spinor condensates

GP equations:

$$-\frac{\hbar^2}{2m_1} \nabla^2 \psi_1 + V_1(\mathbf{r})\psi_1 + U_{11}|\psi_1|^2\psi_1 + U_{12}|\psi_2|^2\psi_1 = \mu_1\psi_1$$

$$-\frac{\hbar^2}{2m_2} \nabla^2 \psi_2 + V_2(\mathbf{r})\psi_2 + U_{22}|\psi_2|^2\psi_2 + U_{12}|\psi_1|^2\psi_2 = \mu_2\psi_2$$

equilibrium:  $U_{11} > 0$ ,  $U_{22} > 0$ ,  $U_{11} - \frac{U_{12}^2}{U_{22}} > 0$

$$n_1 = \frac{U_{22}(\mu_1 - V_1) - U_{12}(\mu_2 - V_2)}{U_{11}U_{22} - U_{12}^2}$$

$$n_2 = \frac{U_{11}(\mu_2 - V_2) - U_{12}(\mu_1 - V_1)}{U_{11}U_{22} - U_{12}^2}$$

Thomas-Fermi approx.

$$\begin{aligned} V_1(\mathbf{r}) &= m_1\omega_1^2 r^2/2 \\ V_2(\mathbf{r}) &= m_2\omega_2^2 r^2/2 \end{aligned} \quad n_2 = \frac{\mu_2}{U_{22}} \left(1 - \frac{r^2}{R_2^2}\right)$$



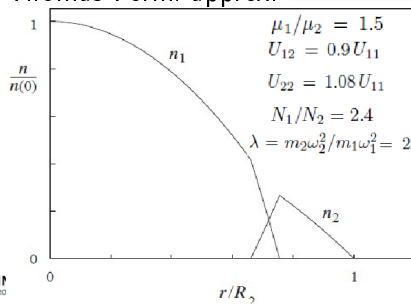
# Spinor condensates

$$n_1 = \frac{U_{22}(\mu_1 - V_1) - U_{12}(\mu_2 - V_2)}{U_{11}U_{22} - U_{12}^2}$$

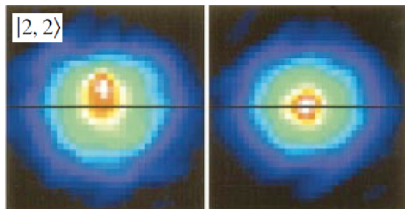
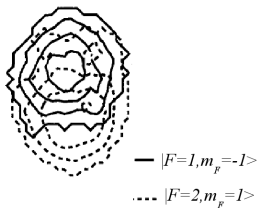
$$n_2 = \frac{U_{11}(\mu_2 - V_2) - U_{12}(\mu_1 - V_1)}{U_{11}U_{22} - U_{12}^2}$$

$$\begin{aligned} V_1(r) &= m_1\omega_1^2 r^2/2 \\ V_2(r) &= m_2\omega_2^2 r^2/2 \end{aligned} \quad n_2 = \frac{\mu_2}{U_{22}} \left(1 - \frac{r^2}{R_2^2}\right)$$

Thomas-Fermi approx.

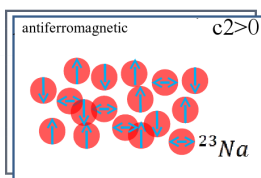
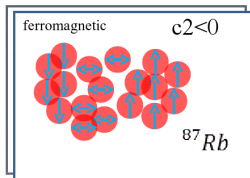


# Spinor condensates

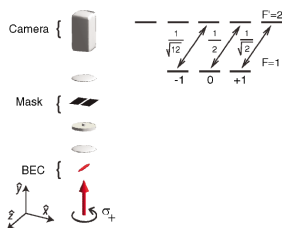


# Spinor condensates - spin domains

$$c_2 = 4\pi\hbar^2(a_2 - a_0)/3m$$



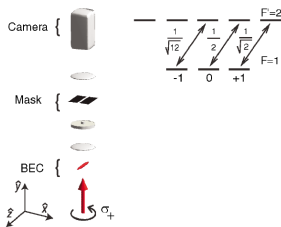
# Spinor condensates - spin domains



- $^{87}\text{Rb}$  BEC is prepared in the dipole trap in the  $|F=1, m_F=0\rangle$  state
- spin dependent energy per particle:  
 $c_2 n \langle \vec{\hat{F}} \rangle^2 + q \langle \hat{F}_z \rangle^2$ , where  $\vec{\hat{F}}$  denotes the dimensionless spin vector operator.
- $c_2 = (4\pi\hbar^2/3m)(a_2 - a_0) < 0$  and  $q = (h \times 70 \text{ Hz/G}^2) B^2$  is the quadratic Zeeman shift
- BEC is prepared at a high quadratic Zeeman shift ( $q \gg 2|c_2|n$ )
- By rapidly reducing the magnitude of the applied magnetic field, the system is quenched to conditions in which the ferromagnetic phase is energetically favored ( $q \ll 2|c_2|n$ )
- At variable times  $T_{hold}$  after the quench, high-resolution maps of the magnetization vector density were obtained using magnetization - sensitive phase contrast imaging



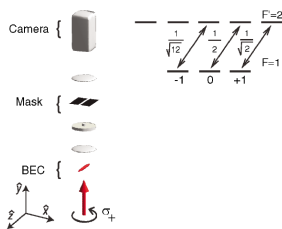
# Spinor condensates - spin domains



- $^{87}\text{Rb}$  BEC is prepared in the dipole trap in the  $|F=1, m_F=0\rangle$  state
- spin dependent energy per particle:  
 $c_2 n \langle \vec{F} \rangle^2 + q \langle \hat{F}_z^2 \rangle$ , where  $\vec{F}$  denotes the dimensionless spin vector operator.
- $c_2 = (4\pi\hbar^2/3m)(a_2 - a_0) < 0$  and  $q = (h \times 70 \text{ Hz/G}^2) B^2$  is the quadratic Zeeman shift
- BEC is prepared at a high quadratic Zeeman shift ( $q \gg 2|c_2|n$ )
- By rapidly reducing the magnitude of the applied magnetic field, the system is quenched to conditions in which the ferromagnetic phase is energetically favored ( $q \ll 2|c_2|n$ )
- At variable times  $T_{hold}$  after the quench, high-resolution maps of the magnetization vector density were obtained using magnetization - sensitive phase contrast imaging



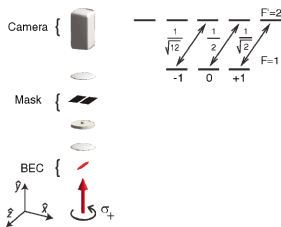
# Spinor condensates - spin domains



- $^{87}\text{Rb}$  BEC is prepared in the dipole trap in the  $|F=1, m_F=0\rangle$  state
- spin dependent energy per particle:  
 $c_2 n \langle \vec{F} \rangle^2 + q \langle \hat{F}_z^2 \rangle$ , where  $\vec{F}$  denotes the dimensionless spin vector operator.
- $c_2 = (4\pi\hbar^2/3m)(a_2 - a_0) < 0$  and  $q = (h \times 70 \text{ Hz/G}^2) B^2$  is the quadratic Zeeman shift
- BEC is prepared at a high quadratic Zeeman shift ( $q \gg 2|c_2|n$ )
- By rapidly reducing the magnitude of the applied magnetic field, the system is quenched to conditions in which the ferromagnetic phase is energetically favored ( $q \ll 2|c_2|n$ )
- At variable times  $T_{hold}$  after the quench, high-resolution maps of the magnetization vector density were obtained using magnetization - sensitive phase contrast imaging



# Spinor condensates - spin domains

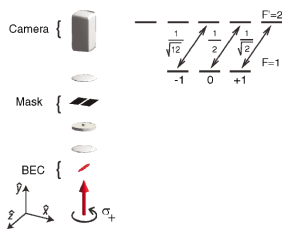


- $^{87}\text{Rb}$  BEC is prepared in the dipole trap in the  $|F=1, m_F=0\rangle$  state
- spin dependent energy per particle:  
 $c_2 n \langle \vec{F} \rangle^2 + q \langle \hat{F}_z \rangle^2$ , where  $\vec{F}$  denotes the dimensionless spin vector operator.
- $c_2 = (4\pi\hbar^2/3m)(a_2 - a_0) < 0$  and  $q = (\hbar \times 70 \text{ Hz/G}^2) B^2$  is the quadratic Zeeman shift
- BEC is prepared at a high quadratic Zeeman shift ( $q \gg 2|c_2|n$ )
- By rapidly reducing the magnitude of the applied magnetic field, the system is quenched to conditions in which the ferromagnetic phase is energetically favored ( $q \ll 2|c_2|n$ )
- At variable times  $T_{hold}$  after the quench, high-resolution maps of the magnetization vector density were obtained using magnetization - sensitive phase contrast imaging





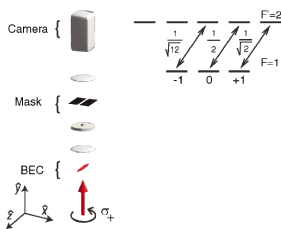
# Spinor condensates - spin domains



- $^{87}\text{Rb}$  BEC is prepared in the dipole trap in the  $|F=1, m_F=0\rangle$  state
- spin dependent energy per particle:  
 $c_2 n \langle \vec{F} \rangle^2 + q \langle \hat{F}_z \rangle^2$ , where  $\vec{F}$  denotes the dimensionless spin vector operator.
- $c_2 = (4\pi\hbar^2/3m)(a_2 - a_0) < 0$  and  $q = (\hbar \times 70 \text{ Hz/G}^2) B^2$  is the quadratic Zeeman shift
- BEC is prepared at a high quadratic Zeeman shift ( $q \gg 2|c_2|n$ )
- By rapidly reducing the magnitude of the applied magnetic field, the system is quenched to conditions in which the ferromagnetic phase is energetically favored ( $q \ll 2|c_2|n$ )
- At variable times  $T_{\text{hold}}$  after the quench, high-resolution maps of the magnetization vector density were obtained using magnetization - sensitive phase contrast imaging



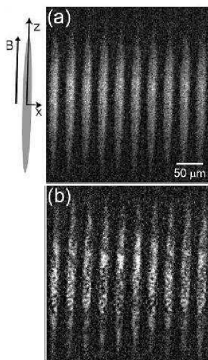
# Spinor condensates - spin domains



- $^{87}\text{Rb}$  BEC is prepared in the dipole trap in the  $|F=1, m_F=0\rangle$  state
- spin dependent energy per particle:  
 $c_2 n \langle \vec{F} \rangle^2 + q \langle \hat{F}_z \rangle^2$ , where  $\vec{F}$  denotes the dimensionless spin vector operator.
- $c_2 = (4\pi\hbar^2/3m)(a_2 - a_0) < 0$  and  $q = (h \times 70 \text{ Hz}/G^2)B^2$  is the quadratic Zeeman shift
- BEC is prepared at a high quadratic Zeeman shift ( $q \gg 2|c_2|n$ )
- By rapidly reducing the magnitude of the applied magnetic field, the system is quenched to conditions in which the ferromagnetic phase is energetically favored ( $q \ll 2|c_2|n$ )
- At variable times  $T_{hold}$  after the quench, high-resolution maps of the magnetization vector density were obtained using magnetization - sensitive phase contrast imaging



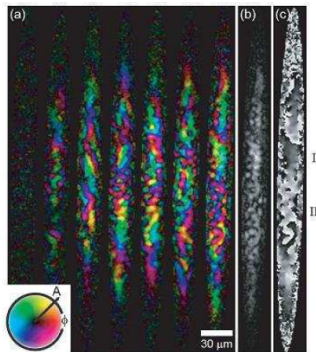
# Spinor condensates - spin domains



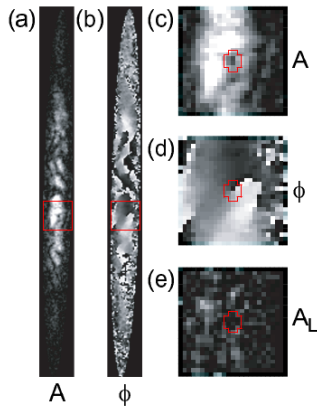
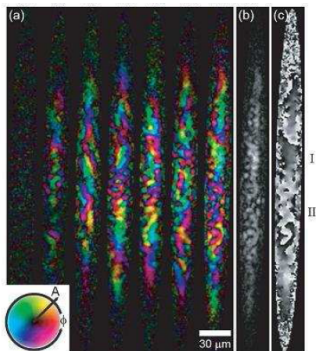
- $^{87}\text{Rb}$  BEC is prepared in the dipole trap in the  $|F = 1, m_F = 0\rangle$  state
- spin dependent energy per particle:  
 $c_2 n \langle \vec{F} \rangle^2 + q \langle \hat{F}_z^2 \rangle$ , where  $\vec{F}$  denotes the dimensionless spin vector operator.
- $c_2 = (4\pi\hbar^2/3m)(a_2 - a_0) < 0$  and  $q = (h \times 70\text{Hz}/G^2)B^2$  is the quadratic Zeeman shift
- BEC is prepared at a high quadratic Zeeman shift ( $q \gg 2|c_2|n$ )
- By rapidly reducing the magnitude of the applied magnetic field, the system is quenched to conditions in which the ferromagnetic phase is energetically favored ( $q \ll 2|c_2|n$ )
- At variable times  $T_{\text{hold}}$  after the quench, high-resolution maps of the magnetization vector density were obtained using magnetization - sensitive phase contrast imaging



# Spinor condensates - spin domains



# Spinor condensates - spin domains



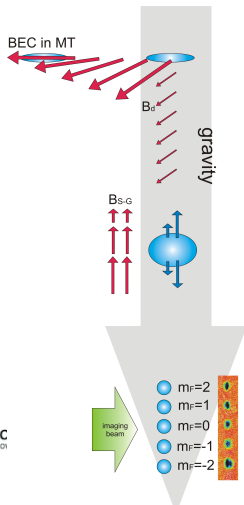
# Stern-Gerlach detection

The field of the magnetic trap is adiabatically replaced by a homogeneous, weak magnetic field  $B_d$  in a given direction.

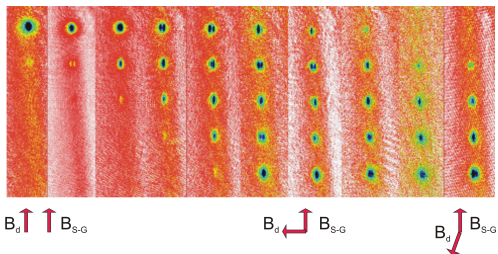
Atoms start to fall freely under gravity and their spins follow the magnetic field direction.

After a given time of free fall expansion (1-20 ms), the MT field is nonadiabatically pulsed for duration of 1-2 ms. The atomic spins are projected on the direction of the strong gradient of the magnetic field ( $B_{SG}$ ).

The Stern-Gerlach force separates the condensates.



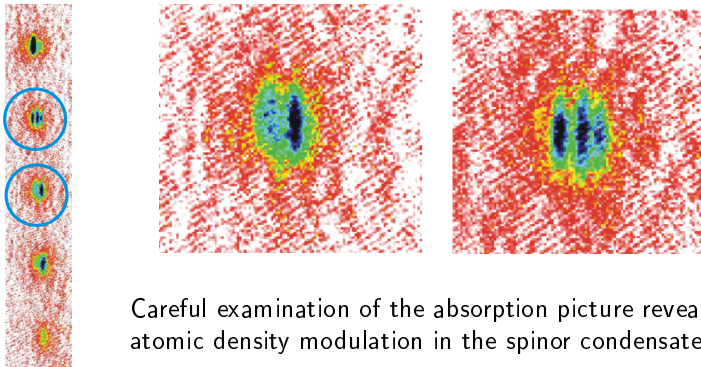
# Population control



Absorption images of the spinor condensates expanded by the Stern-Gerlach force taken for different orientation of the  $B_d$  vs the  $B_{S-G}$  field.



## Spatial modulation – spinor domains

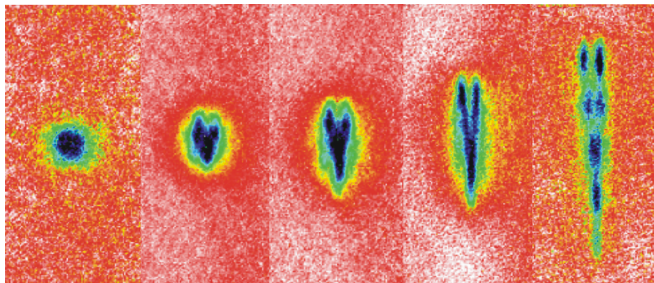


Careful examination of the absorption picture reveals atomic density modulation in the spinor condensates.





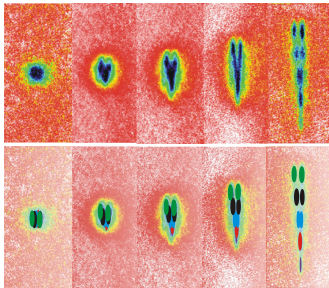
## Spatial modulation – spinor domains



Absorption images of the spinor condensates taken during their separation after the Stern-Gerlach pulse.



## Spatial modulation – spinor domains



The spatial modulation of the spinor condensates is most likely caused by the presence of spin domains

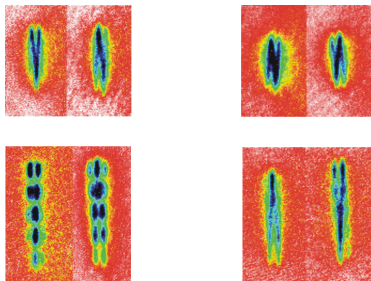


before the  $B_{SG}$  field.  
INNOWACYJNA GOSPODARKA  
NARODOWA STRATEGIA SPÓJNOŚCI

UNIA EUROPEJSKA  
EUROPEJSKI FUNDUSZ  
ROZWOJU REGIONALNEGO



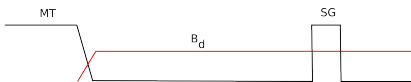
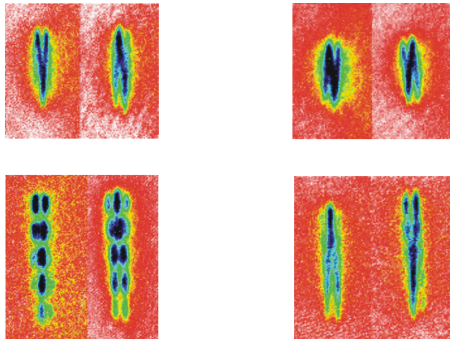
## Spatial modulation – spinor domains



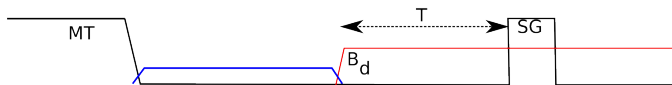
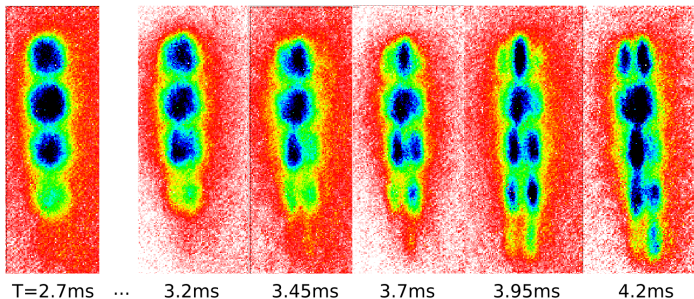
The modulation, i.e. the position of spin domains varies under constant experimental conditions.



# Spatial modulation instability – preliminary results



## Spatial modulation – spinor domains

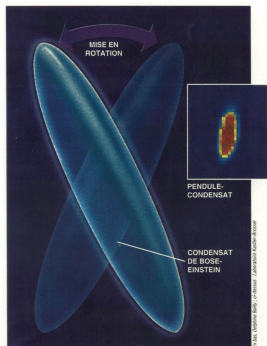


## Collective oscillations (cigar trap)

|                  | BEC<br>superfluid        | ideal gas<br>collisional    | ideal gas<br>collisionless |
|------------------|--------------------------|-----------------------------|----------------------------|
| m=0<br>radial    | $2\omega_{\perp}$        | $\sqrt{10/3}\omega_{\perp}$ | $2\omega_{\perp}$          |
| m=0<br>axial     | $\sqrt{5/2}\omega_z$     | $\sqrt{12/5}\omega_z$       | $2\omega_z$                |
| m=2,-2<br>radial | $\sqrt{2}\omega_{\perp}$ | $\sqrt{2}\omega_{\perp}$    | $2\omega_{\perp}$          |



# Scissors mode



Scissors mode above  $T_c$ : the gas oscillates with frequencies  $\omega_x \pm \omega_y$

Scissors mode below  $T_c$ : the superfluid oscillates with frequency  $\sqrt{\omega_x^2 + \omega_y^2}$



# Mott insulator - superfluid transition

